NAVIGATION: *Journal of The Institute of Navigation*
Vol. 22, No. 3, Fall 1975
Printed in U.S.A.

Accuracy Specifications for Automatic Omega Navigators

F. C. SAKRAN, JR.

Abstract

FULLY AUTOMATIC OMEGA NAVIGATION SYSTEMS have been demonstrated and are beginning to be used operationally in aircraft and other vehicles. A natural question is the accuracy achieved by such systems. Concern over the probability of maintaining correct lane identification complicates this question. Use of the root-mean-square (rms) statistics is shown to be a misleading measure of operational performance. Alternate methods of specifying the navigational errors of automatic Omega navigators are discussed. Cumulative percentile plots are recommended for the specification of errors. Use of Weibull probability paper to study radial error trends is demonstrated. Illustrations of error analysis techniques are given, based on actual Omega flight test data.

Introduction

With the appearance of reliable Omega signal fields covering an increasing area of the earth, more and more craft will be considered as candidates for an Omega navigation capability. Most of the Omega navigation equipment manufactured to date has been of a non-automatic nature, requiring user corrections for propagation effects and manual plotting of phase measurements on specially prepared charts. In future applications, particularly those in aviation, emphasis will be on automatic Omega navigation systems, which combine receiving circuitry with digital processors and provide automatic compensation for diurnal propagation effects and coordinate conversion. The user is provided a present position readout directly in geographical map coordinates, such as latitude and longtitude. This paper considers some aspects of the measurement and specification of geographic position fix accuracy with regard to automatic Omega navigation equipments.

The author is with the U. S. Naval Air Test Center, Patuxent River, MD 20670. He presented this paper at the Second Omega Symposium in Washington, D.C. on Nov. 7, 1974.

Accuracy Specification Goals

In some respects the problem of Omega accuracy specification is similar to that of other automatic navigation devices. However, it will be shown that interpretation of some of the simpler error specifications becomes more difficult in the case of Omega navigators. This difficulty arises because of the presence of error modes which are peculiar to Omega. In inertial and Doppler systems, for instance, so-called "blunder" errors may be caused by false position initializations or updates, grossly erroneous instrument calibration, out-and-out equipment malfunctions, and operator errors. Automatic Omega systems are also susceptible to blunder from these and other sources. A blunder mode unique to Omega is false lane identification or lane slips. Lane slips are evidenced by position offsets at multiples of 6 to 8 nautical miles (nmi). Success in lane keeping is primarily a function of receiver software sophistication and use of other navigational information (in addition to Omega) and thus may vary with equipment design and installation. Maintenance of correct lane count under all operational conditions appears to be one of the major design challenges in automatic Omega systems and thus should be emphasized in performance specifications.

A second large-error mechanism unique to

Omega concerns unpredictable propagation anomalies such as sudden ionospheric disturbance (SID) and polar cap absorption (PCA) events, both of which can cause abnormally large position fix errors. It is widely recognized that the ultimate accuracy of any ordinary Omega geographic position fix is limited by random variations in signal propagation. However, propagation variations will not affect all automatic Omega systems equally, as differing weightings of stations and/or frequencies, measurement fix geometries, and diurnal propagation prediction models will yield differing position fix accuracies even though operating simultaneously at a given location. Propagation disturbances are one cause of mistaken lane count. Fortunately, there seem to be ways in which automatic Omega systems can recognize and, to some degree, minimize the effects of SID's and PCA's through signal comparison, editing and filtering schemes. Severe precipitation static interference can degrade Omega phase tracking, additionally degrading position accuracy. Fortunately for the operational user, severe SID's, PCA's and p-static appear to be relatively rare phenomena. Unfortunately for the equipment test agency, their occurrence is most difficult to predict or to control. Since a practical test program is limited in scope, it may or may not sample system performance under the influence of SID's, PCA's and p-static. Accuracy specifications derived from a test program should recognize the uncontrollable nature of these phenomena.

The previous errors pertain to the actual performance of the Omega equipment. When testing the equipment in an operational environment, additional errors can arise in the test methodology. Even under controlled conditions, problems in position reference datum and in data recording can compromise the results of a navigational accuracy test. For instance, in recent airborne Omega test programs, we have used digital recording equipment along with continuous ground radar tracking for the aircraft position datum reference. This is a relatively reliable (and costly) test methodology. Yet over half of the data analysis effort was spent in identifying and editing out the infrequent instrumentation and radar position datum errors occurring in the data record, so that these errors would not confuse the measured accuracy of the Omega systems being tested.

It would be advantageous to specify the design performance accuracy of a system in the manner most immune to errors arising in test methods. In the following, several measures of navigational accuracy are discussed. The data used as an illustrative example is a small portion (one flight) of that collected during a recent test program at the U. S. Naval Air Test Center.

The Root-Mean-Square, Mean and Median Measures of Sample Accuracy

Stability of the Omega signal field has been described by the root-mean-square (rms) error statistics; e.g., the familiar "One nmi by day, two by night, rms". The rms statistic has also been used in predicting performance of automatic Omega navigators (1). Use of the rms has been justified by a "golden rule" of errors—the effect of a random error is proportional to the square of its size (2). Another way of justifying the rms value is by the Pythagorean Theorem. Consider a population (of size n) of the error variate x_1, x_2, $\cdots x_n$. The rms of x is defined as the positive square root of the second moment about the origin, namely

$$rms\ (x) = \sqrt{\frac{1}{n}\sum x_i^2}$$

Through algebraic manipulation this may be expanded as

$$rms(x) = \sqrt{\mu_x^2 + \sigma_x^2}$$

where

$$\mu_x = \frac{1}{n}\sum x_i$$

and

$$\sigma_x = \sqrt{\frac{1}{n}\sum (x_i - \mu_x)^2}$$

The two quantities under the radical can be recognized as the squares of the population's mean and standard deviation. In a one-dimensional navigation system the mean error represents a bias or offset which, if known, could theoretically be removed by calibration. The standard deviation is a measure of scatter or predictability in the system's error behavior. The rms neatly combines both the mean and the standard deviation by the right triangle relation shown in Fig. 1. While it is of interest to the en-

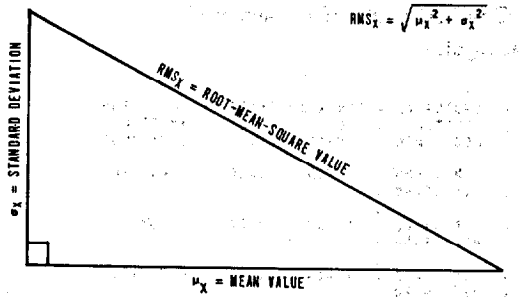

Fig. 1—Relation between the mean, standard deviation and root-mean-square measures of the distribution of a variate x.

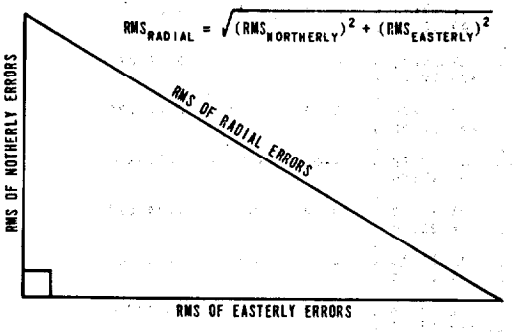

Fig. 2—Relation between the root-mean-square values of northerly, easterly and radial errors in a position fix.

gineer or the quality control inspector to separate a system's error into components of mean and standard deviation, the navigator may not appreciate the difference (especially if he is lost). Intuitively, then, the rms(x) value serves as a practical single measure of the system's error in the x direction. Now if the rms errors of two one-dimensional systems, each navigating at right angles (e.g., northerly and easterly), are combined as the sides of another right triangle, the hypotenuse of this triangle is identical to the rms value of the total (radial) error in the two-dimensional position fix, Fig. 2.

While the population rms error value is operationally meaningful, it can be difficult to approximate with confidence by a sample rms. As an example, Table 1 gives the data sample obtained on what may be a typical "low budget" Omega navigation test flight. The aircraft was flown at low level over a course defined by identifiable landmarks of known surveyed coordinates. The pilot visually estimated when the aircraft was directly over each checkpoint, at which time the Omega system's position display was locked and logged. While this type of flight test is not as well controlled as desired, it is easy to do, is of minimum cost, and yields answers with almost zero delay for data processing. A total of 22 data points was obtained over the 2.6 hour flight; the errors are graphed in Fig. 3. The sample rms of radial error in these 22 samples is 1.08 nmi. Examination of the last two data points shows that they do not follow the trend of the previous 20 points. The reason was not determined. If these two data samples are discarded (or assume only that the test terminated 8 minutes earlier), the rms of the remaining 20 samples drops to 0.75 nmi, a 44 percent change with a 10 percent difference in sample size. This demonstrates a difficulty in comparing rms error values calculated from different test samples.

The rms is very sensitive to infrequent but large blunder errors, such as lane slips. Figure 4 shows how the rms value becomes increasingly sensitive to lane slips as the design accuracy of the system improves. By design accuracy, we mean the basic navigational accuracy of the system exclusive of lane slips or other blunder errors. Existing automatic Omega navigator designs have shown lane slip probabilities of approximately two percent when tested against the existing interim signal field (3). Figure 4 shows that a 1.5 nmi sample rms would result from a system designed to 1.0 nmi rms but degraded by a two percent lane slip probability. A 1.5 nmi rms specification could also be met by a 0.5 nmi rms design system which lost lane count 3.1 percent of the time. The lower curve indicates a maximum allowable lane slip probability of 3.5 percent if an otherwise perfect (zero design error) system were to be rated at 1.5 nmi rms.

Suppose that the 22 sample points of Table 1 are combined with another 22 sample points all of zero error. Now we have a system giving zero error half the time. The new sample rms error value drops only to 0.76 nmi—or takes 22 zero error sample points to have the same effect on the rms as the two higher error points. While the rms has some validity in specifying the largest errors, it gives limited insight into overall systems performance.

There are measures of the central tendency of error which are less sensitive to large blunder

Table 1—Reduced Data Log for One Test Flight of an Automatic Omega Navigator

ACTUAL GEODETIC POSITION HOURS GMT ELPSD	LATITUDE LONGITUDE DEG MIN SEC	INDICATED POSITION DEG MIN	ERROR IN INDICATED POSITION NORTH (NMI)	EAST (NMI)	RADIAL (NMI/DEG)
1938 0.00	35 18 15.0	35 14.60	0.35	0.19	0.40/028
NORMAN,OKLA VOR VISUAL	-97 26 50.0	-97 26.60			
1945 0.12	34 44 32.0	34 44.00	-0.53	-0.27	0.60/207
PAULS VALLEY,OKLA NO VISUAL	-97 16 10.0	-97 16.50			
1952 0.23	34 17 57.6	34 17.30	-0.66	0.36	0.75/151
SPRINGTON,OKLA VISUAL	-97 8 31.8	-97 8.10			
1954 0.27	34 12 41.3	34 12.50	-0.19	0.15	0.24/141
ARDMORE,OKLA VISUAL	-97 10 8.9	-97 9.90			
2011 0.55	33 16 59.0	33 17.30	0.32	-0.10	0.33/343
BLUE RIDGE,VORTAC VISUAL	-96 21 53.0	-96 22.00			
2019 0.68	32 45 18.0	32 45.40	0.10	0.14	0.17/054
TERRELL,TEXAS VISUAL	-96 16 58.0	-96 16.80			
2023 0.75	32 27 52.0	32 28.40	0.53	0.20	0.57/020
SCURRY TEXAS VISUAL	-96 20 14.0	-96 20.00			
2028 0.83	32 6 53.0	32 7.00	0.12	0.24	0.27/064
CORSICANA,TEXAS VISUAL	-96 27 47.0	-96 27.50			
2040 1.03	31 39 41.8	31 40.70	0.87	0.19	0.89/011
WACO,TEXAS VORTAC VISUAL	-97 16 7.5	-97 15.90			
2056 1.30	31 14 4.5	31 15.00	0.92	0.25	0.96/015
LORETA,TEXAS VISUAL	-98 32 11.6	-98 31.90			
2109 1.52	31 51 18.0	31 51.50	0.20	0.04	0.20/012
COLEMAN,TEXAS VISUAL	-99 25 45.0	-99 25.70			
2116 1.63	32 14 8.2	32 14.70	0.56	-0.10	0.57/350
TUSCOLA,TEXAS VISUAL	-99 48 59.1	-99 49.10			
2117 1.65	32 20 10.0	32 20.50	0.33	-0.45	0.56/306
DYESS,TEXAS VISUAL	-99 50 4.0	-99 50.60			
2119 1.68	32 28 52.5	32 29.30	0.42	-0.35	0.55/320
ABILENE,TEXAS VISUAL	-99 51 47.1	-99 52.20			
2125 1.78	32 55 52.0	32 56.80	0.83	0.04	0.83/002
STAMFORD,TEXAS VISUAL	-99 47 9.0	-99 47.10			
2137 1.98	33 46 41.5	33 47.50	0.81	-0.21	0.83/345
GUTHRIE,TEXAS VORTAC VISUAL	-100 20 8.9	-100 20.40			
2146 2.13	34 18 58.0	34 19.90	0.93	-0.40	1.01/336
GUANAH,TEXAS VISUAL	-99 44 49.0	-99 45.30			
2152 2.23	34 31 10.1	34 32.10	0.93	-0.27	0.97/343
ALTUS,OKLA NO VISUAL	-99 16 28.4	-99 16.80			
2157 2.32	34 51 59.5	34 53.30	1.31	-0.34	1.35/345
HOBART,OKLA VISUAL	-99 3 46.9	-99 4.20			
2209 2.52	35 1 50.0	35 2.90	1.07	-0.34	1.12/343
CHICKASHAW,OKLA VISUAL	-97 56 11.0	-97 56.60			
2214 2.60	35 14 15.0	35 13.30	-0.95	2.40	2.58/111
NORMAN,OKLA VISUAL	-97 26 50.0	-97 25.90			
2217 2.65	35 34 1.1	35 32.90	-1.12	2.55	2.78/113
TINKER,OKLA VISUAL	-97 22 43.0	-97 19.60			

errors than is the rms. The sample mean and median are well-known examples. The sample mean is linearly influenced by large blunder errors such as lane slips, as is shown in Fig. 4. The sample mean is also influenced by extreme values and sample size: the sample mean of the 22 test points in Table 1 drops from 0.85 nmi to 0.67 nmi with deletion of the last two data points. But if the sample were augmented by the additional 22 zero-error points, the new sample mean drops only to 0.43 nmi. Like the rms, the mean does not show how good a system can be when the system

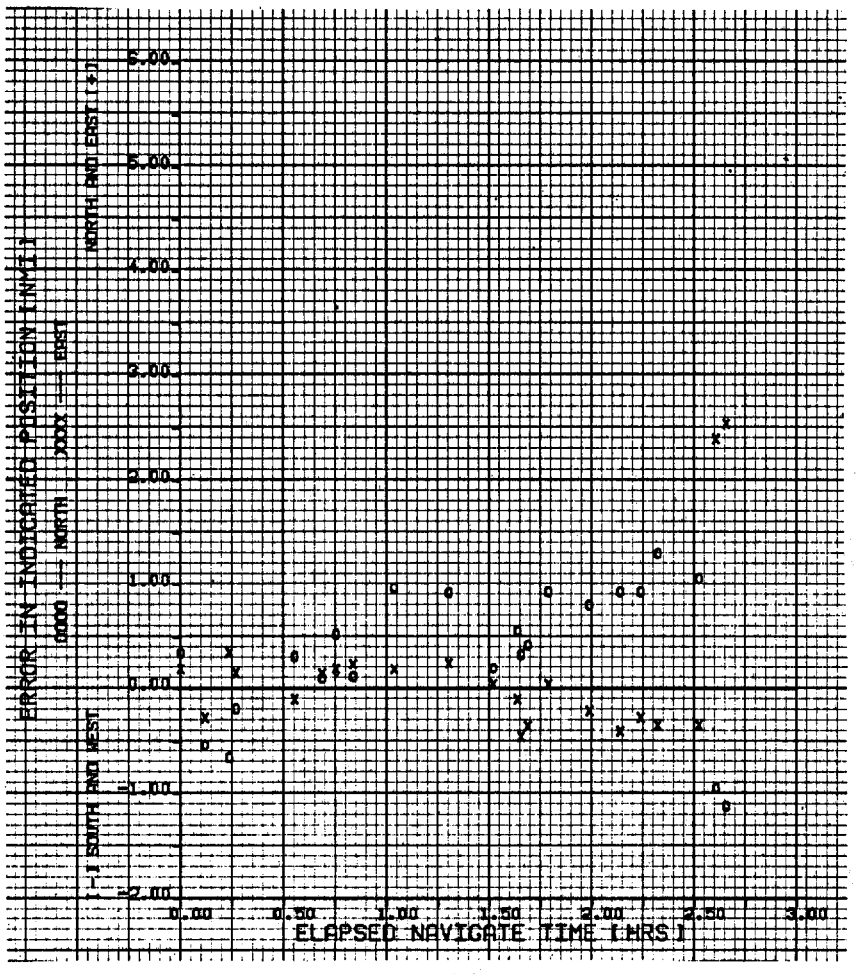

Fig. 3—Time history graph of errors in the Omega position fixes logged in Table 1.

is sometimes, although seldom, in error. The sample median, on the other hand, is a very insensitive measure of central tendency. It is statistically robust, but inefficient. So much so, in fact, that it is absolutely unaffected by lane slip blunder until the occurrence of blunder reaches 50 percent. After all, the numerical value of the sample median is completely determined by one or, at most, two sample points. The median is also the measure least sensitive to small changes in sample size: the median of radial errors listed in Table 1 drops from 0.67 nmi to 0.58 nmi with deletion of the last two sample points. However, adding 22 zero-error points drops the sample median to 0.09 nmi.

Separate specifications for design accuracy and for maximum probability of false lane count are desirable. They will depend on the intended application of the equipment. For an automatic Omega navigation system intended to stand alone as a general purpose geographic position fixing aid, design accuracy may very well be relaxed in order to achieve maximum reliability of correct lane count. On the other hand, Omega measurements used to augment an inertial navigation system may be required to a higher degree of design accuracy, but with gross lane slip errors being more tolerable than moderate errors since the former may be easily detectable and resettable by comparison with the continuous inertial

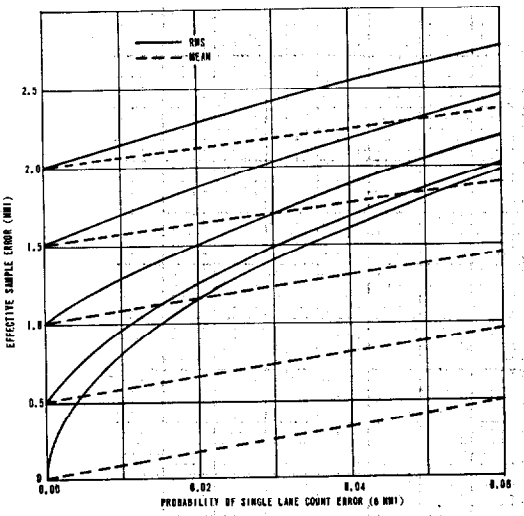

Fig. 4—Curves showing how the sample root-mean-square and mean measures of position error change when lane count (8 nmi) errors occur. Note particularly how strongly the rms is affected by infrequent lane count errors when error is otherwise low.

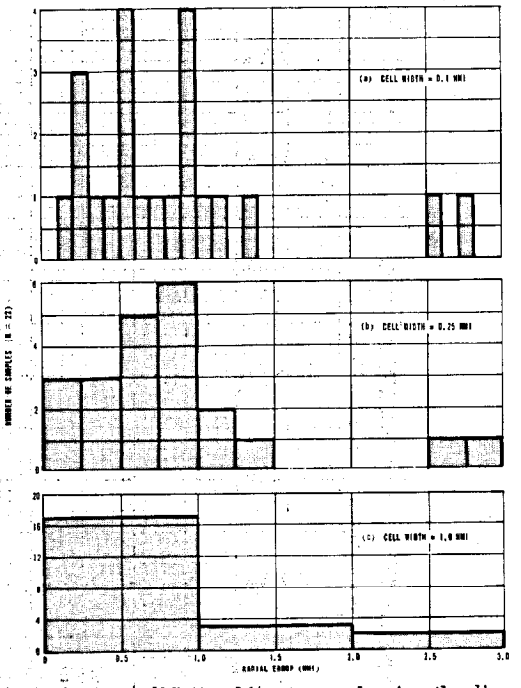

Fig 5—Three different histograms showing the distribution of radial error in the 22 position fixes given in table 1. Samples have been grouped into cells of width (a) 0.1, (b) 0.25 and (c) 1.0 nmi.

measurements. None of the mean, median or rms measures of position error provide sufficient information to specify Omega system accuracy fully, as these measures give no clues as to the statistical distribution of error.

Sample Distributions

By dividing the range of error values into cells (class intervals) and plotting the number of samples occurring in each cell range, the familiar histogram results. The histogram presentation gives an easy-to-interpret idea of the distribution of the sample error values. As the sample size increases, the histogram approaches a plot of the probability density function (pdf) representing the parent population from which the sample was drawn. Unfortunately a given sample does not result in a unique histogram. Figure 5 gives three histograms, all derived from the sample data of Table 1, but with different cell widths along the error scale. On the basis of 5.a we might decide either to discard the two outlying data points as "bad data" or to model them as a secondary error mode. On the other hand, we might conclude our 22 points are a sparse sample from a single population conforming to either a Rayleigh-like distribution (5.b) or an exponential distribution (5.c).

Just as the parent population's cumulative distribution function (CDF) is the integral of the population's pdf, the summation of ranked sample points can be plotted as an approximation of the CDF. The cumulative sample percentile graph is a monotonically increasing function which approaches a smooth S-shaped curve as sample size increases. Unlike the histogram, this plot is uniquely determined by the 22 data points as shown in Fig. 6. The cumulative sample percentile curve weights each sample point equally without regard to its magnitude. Occasional large error samples do not strongly affect the lower percentile error estimates. The cumulative distribution of the truncated 20 point sample is also shown in Fig. 6. It conforms closely to the 22 point sample to over the 85th percentile level. Note particularly the close agreement of the two samples at the 50th percentile level (the median). This again points out the robustness of the median as a sample statistic. The radial error sample median is the most robust estimate of the population circular probable error, or CEP. The CEP is defined as the radius

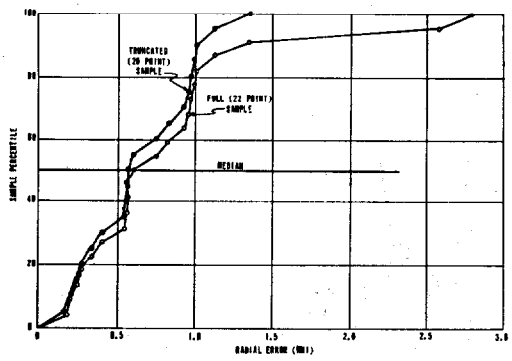

Fig 6—Cumulative percentiles of radial position error in the data sample given in table 1 plotted on linear graph paper. Note close agreement of the full 22 point and the truncated 20 point samples at the 50th percentile (median) level.

of a circle centered at the actual position, which includes 50 percent of the navigation system's position fixes. From a CEP specification a navigator knows that his system will be in error by less than the CEP value half of the time. He has no clue as to how bad errors will be the other half of the time unless information about the population distribution is also provided. The cumulative sample percentile curve provides information about the error distribution in a simple and easy-to-interpret manner. Note that no assumptions have been made concerning the statistical model describing the system's error population.

Models for Position Error Population Distributions

When extrapolating a test sample to the sample's parent population, a knowledge of the population's statistical distribution is desirable. If a mathematical model of the distribution function may be assumed, its parameters may then be estimated from the data sample and future performance predicted with higher efficiency than if such a priori information were not available. The most meaningful quantity with which to specify Omega position fix accuracy to the practicing navigator is the radial error expected in the position fix. The problem of deriving a model for the statistical distribution of radial position error has been extensively studied, and many solutions of expected radial error percentile levels have been proposed. Practically all of these derivations begin with the assumption that the position fix is determined by the crossing of (only) two orthogonal lines of position (LOP) with the errors in each LOP being uncorrelated and normally distributed and require that the error population means and standard deviations for each LOP be estimated from sample data. None of the assumptions applies directly to the Omega position fix, which is susceptible to geometrical errors from non-orthogonal LOP crossing angles, correlated propagation-related errors in each LOP, and (especially in automatic sets) possible overdetermination of position by more than two LOP measurements. If the error in each phase measurement can be assumed to be normally distributed, these limitations can be removed by a transformation of variables (4). The transformation results in an error scatter pattern which is elliptical and which follows a general bivariate normal probability density. Several approximate solutions for the distribution of radial error in a bivariate normal population are available, (4)–(6). (In the particular case of a priori knowledge of a circular normal (Rayleigh) distribution of errors, an exact solution of the radial error distribution can be obtained. The circular normal case results from assuming the two LOP's to be orthogonal at the fix site and errors in the LOP's to be uncorrelated and have zero means and equal standard deviations.) When experimental performance data does conform to a normal error distribution, these approximations serve well. But since the standard deviations estimates are strongly influenced by outlying sample points, the radial error estimates are also sensitive to wild data. Figure 7 compares the standard deviation (one-sigma) contours of bivariate normal densities fitted to the data sample of Table 1, with and without the last two data samples. The influence of the two outlying points is easily seen in the size, position, and orientation of the 22-point ellipse, which does not conform to the scatter of the majority of the data points. CEP circles estimated from the fitted bivariate normal distributions (5) are also shown. Including the two outlying sample points raises the CEP estimate from 0.58 to 0.87 nmi, three times the change seen in the sample median.

The Weibull Distribution as a Model of Omega Radial Error

Several models for directly estimating radial error have been proposed for use in navigation

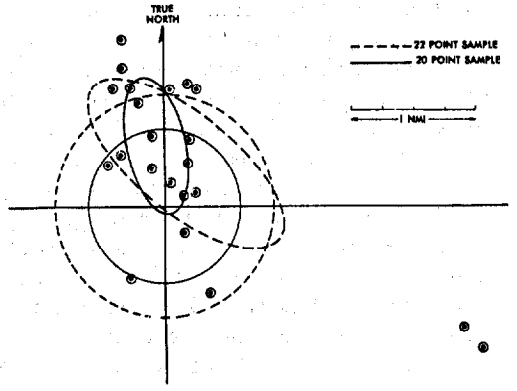

Fig. 7—One-sigma elliptical contours and CEP circles of bivariate normal distributions fitted to (a) the 22 point data sample, and (b) the 20 point truncated sample. Note the strong influence of the two sample points outlying to the southeast.

system evaluations. Although not justified on a purely theoretical basis, they have proven useful in the analysis of Omega test data. One of these models, the Weibull distribution, will now be described. The Weibull distribution was originally proposed in 1951 (7), to describe various physical phenomena and has become widely accepted as a system failure model in reliability studies. Although the Weibull distribution has been discussed as a model for navigational radial errors (8), its simplicity has not been widely appreciated.

In its two-parameter form, the Weibull cumulative distribution function (CDF) of radial position fix error R ($R > 0$) as

$$CDF(R) = 1 - e^{-(R/B)^C},$$ where B and C are arbitrary positive constants.

One advantage of the Weibull distribution is that the parameters provide direct insight into the radial error distribution. The "scale parameter" B, in units of length, characterizes the magnitude of the error. More exactly, B is the radius of a circle centered at the origin which encloses 63.2 percent of the errors. The "shape parameter" C, which is dimensionless, describes the spread or uniformity of the error density. Thus, the parameters are somewhat analogous (but not identical to) mean and standard deviation in a single-axis distribution. For $C \leq 1$, the mode or most probable error value equals zero; for $C > 1$, the mode approaches B units of radial error. The range of B and C values results in a rich variety of pdf

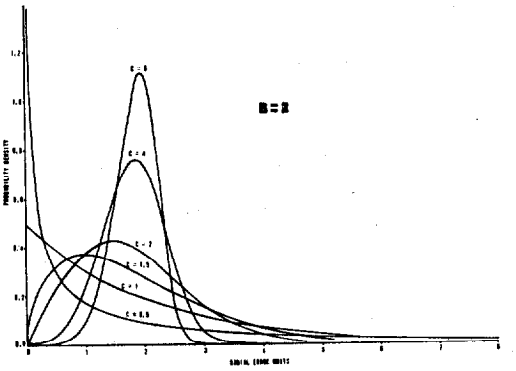

Fig. 8a—Examples of the Weibull probability density function when scale factor = 2 units.

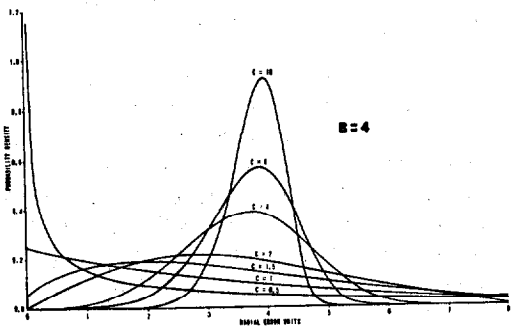

Fig. 8b—Example of the Weibull probability density function when scale factor = 4 units.

shapes, as is shown in Fig. 8. Several well-known distributions are included as special cases of Weibull distributions. For example, if the shape parameter $C = 2$, the Weibull is identical to the circular normal distribution. The corresponding Weibull scale parameter is $B = \sqrt{2}\,\sigma$. For $C = 1$, the Weibull simplifies to the exponential distribution with its more slowly decaying tail. The exponential distribution has been suggested as a description of extreme values of navigational errors (9). Test data for existing automatic Omega navigators has shown values of C ranging from 0.8 to 6.6 for single test runs. Ensembles of several test runs (which sample performance over a range of time and location) have yielded values of C ranging between 1.5 and 2.1 for different equipment designs.

Generalized Weibull probability graph paper can be prepared on which any Weibull CDF will plot as a straight line (10). The advantages of a linear plot include display of intermediate per-

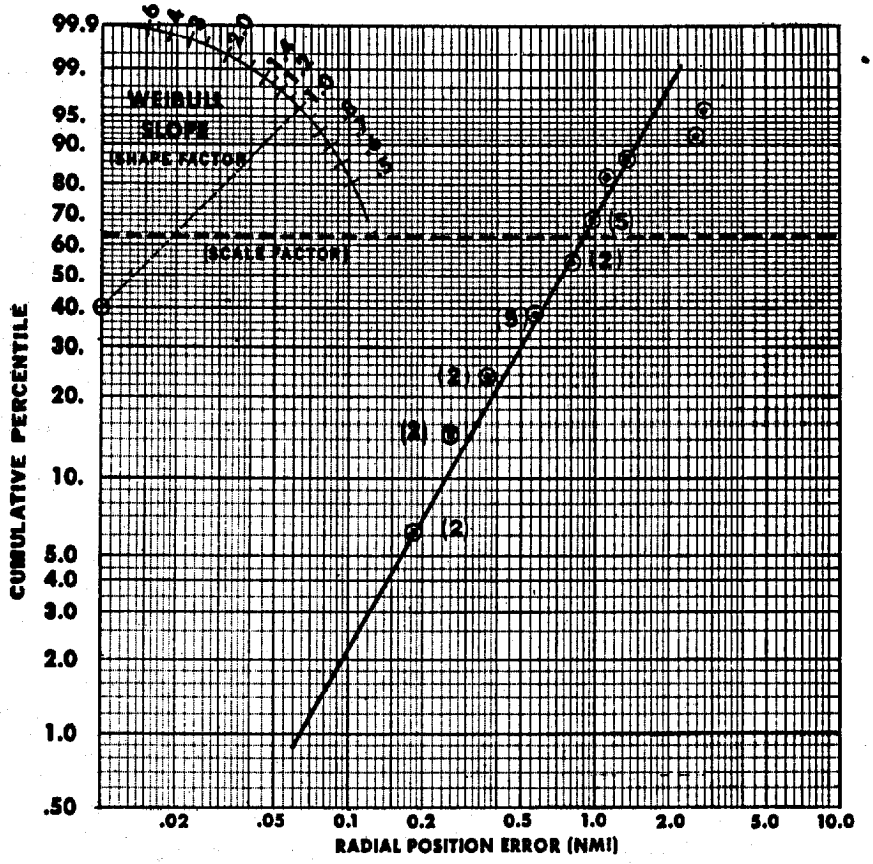

Fig. 9—Cumulative percentiles of the 22 point radial position error sample plotted on Weibull probability paper. Scales are adjusted such that Weibull CDF's graph as a straight line. Numbers in parentheses indicate how many sample points are represented by the mean ranked point plotted (See text).

centile levels, easy assessment of the goodness of fit of the sample data to a particular distribution, and easy comparison of data from two or more test programs. Figure 9 shows the 22 point data sample plotted on Weibull probability paper. The points were plotted using the following procedures:

1. The n sample points of radial error R are first placed in increasing order; i.e., $R_1 \leq R_2 \leq \cdots \leq R_n$.
b. To each sample point R_m is assigned a mean rank percentile $F(R_m)$ where

$$F(R_m) = \frac{m}{n+1} \times 100$$

c. The $F(R_m)$ are plotted vs. R_m on Weibull paper.

d. Where an error value is repeated k times, or k sample points are too close to be plotted without crowding, the k points are grouped. The grouped mth through $m + k$th sample points are plotted as a single point having

$$\text{mean radial error } \frac{1}{k} \sum_{i=m}^{m+k} R_i$$

and group rank percentile $\dfrac{\sqrt{m(m+k)}}{n} \times 100$

The above plotting techniques are discussed in Ref. (11). If the sample conforms exactly to a Weibull distribution, the plotted points will lie on a straight line from which the scale and shape parameters can be determined. In actuality the plotted data will show some scatter. A line can

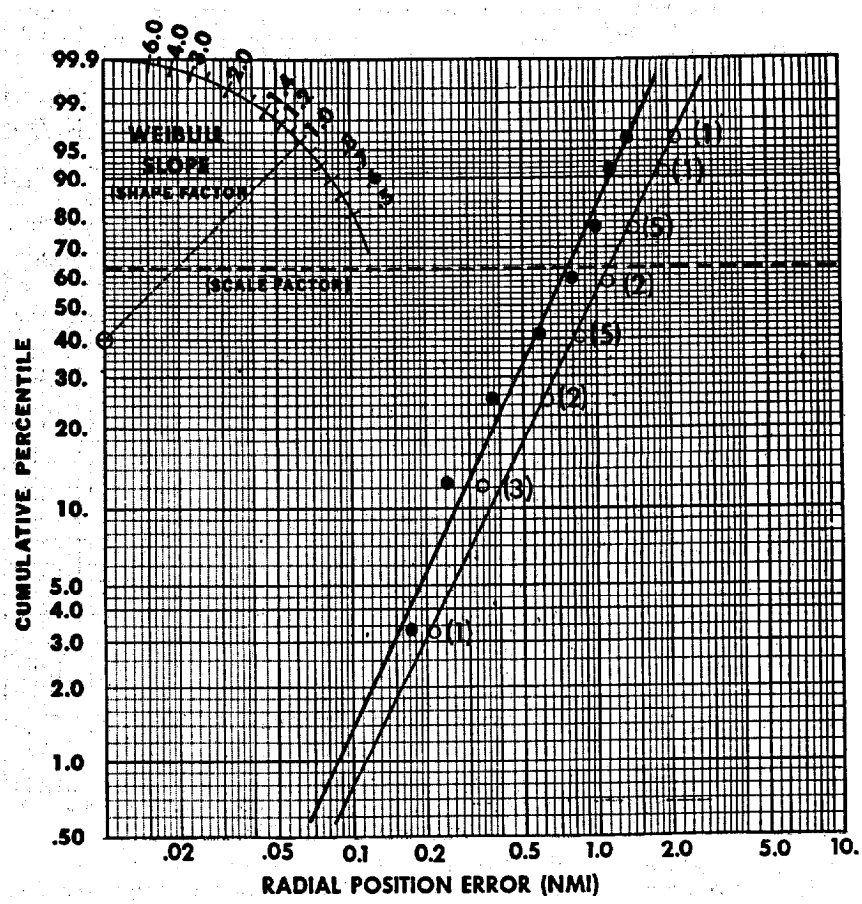

Fig. 10—Comparison of radial error distributions for two different automatic Omega designs. The left line (solid dots) was fitted to the edited 20 point sample of the navigation system previously described. The right line (open circles) was fitted to the equivalent sample of a second navigation system that was tested concurrently. Note the similarity in slopes (Weibull shape parameters) of the two error distributions. Median ranked samples were plotted; numbers in parentheses indicate multiple samples shown as single plotting point.

still be fitted by inspection, although in this case replacement of the mean ranked percentiles by tabulated values of the median ranks is recommended (12). A more repeatable procedure is to determine the scale and shape parameters directly from the numerical sample data. Ref. (13) proposes estimates for B and C which use the transformed variate $\ln(R)$. When applied to the sample of Table 1, they yield $B = 0.92$ nmi and $C = 1.74$. This CDF is shown by the line in Fig. 9, which appears to fit all but the two higher data points. Refitting after deletion of these two points yields $B = 0.75$ nmi and $C = 2.10$ which define a Weibull distribution matching the 20 point sample within 0.1 nmi. This distribution is shown in Fig. 10.

Also shown in Fig. 10 is the Weibull distribution fitted to a second 20 point data sample. This second data is from a different design of automatic Omega navigation set, which was evaluated concurrently and along side the first set. The Weibull parameters fitted to this data are $B = 1.10$ nmi and $C = 2.00$. It is interesting to note the similarity in shape parameters for the two sets which were using the same Omega signals (stations and frequencies) and on-board velocity aids during this particular test flight. The difference in scale parameters clearly shows one set to have

been more accurate in its geographic position fixing than the other.

Conclusions

Omega position fixes are known to be susceptible to error mechanisms such as propagation disturbances and lane slips which can result in infrequent but relatively large errors. An important measure of the performance of an automatic Omega navigator is the success with which the magnitude and/or the probability of large errors is reduced. The rms, mean and median measures of position fix accuracy are inadequate as performance specifications for automatic Omega navigators. The rms of radial error has operational significance to the user of a system. However, the sample rms is unreliable because of its excessive weighting of large sample values which makes test rms values overly sensitive to sample size and to data acceptance/rejection criteria. Neither the rms nor the sample mean indicate the difference between an "always average" system and a "usually exceptional but infrequently bad" system. The radial error sample median, as an estimate of CEP, is a robust and repeatable measure of system accuracy at the 50th percentile level. The user, however, is not satisfied with only a 50th percentile specification, and the CEP of an automatic Omega navigator cannot be confidently extrapolated to the higher percentile levels. Presentation of automatic Omega position errors by cumulative percentiles is recommended as the simplest method of specifying navigational accuracy. The Weibull probability distribution function has shown promise as a robust two-parameter model for radial Omega position fix errors. Plots of radial error samples on Weibull probability paper have proven useful in comparison of different test samples and in identification of outlying data points apparently not part of the dominant error population.

References

1. MIL-N-81678A(AS), "Military Specification, AN/ARN-99(V) Omega Navigation Set", 3 Jan 1974.
2. Anderson, E. W., "The Principles of Navigation", American Elsevier, New York, 1966 (35).
3. Sakran, F. C. Jr., "Final Report", *Technical Evaluations of AN/ARN-99(XN-2) and CMA-719 Omega Navigation Sets in P-3A and P-3B Airplanes*, Nav al Air Test Center, Patuxent River, Md. Report WST-74R-74 of 24 June 1974, AD 921-410L.
4. Swanson, E. R., *Estimating the Accuracy of Navigation Systems*, Naval Electronics Laboratory, San Diego, California, Report 1188 of 24 Oct 1963, AD 427-269.
5. Rosen, L. L. and Harmer, D. L., "Inertial System Performance Evaluation", *Proceedings*, Third Inertial Guidance Test Symposium, Oct. 1966, U. S. Air Force Missile Development Center, Holloman AFB, New Mexico, Report MDC-TR-66-106 (Vol. 1), AD 800-672.
6. Terzian, R. C., "Discussion of 'A Note on CEP's' ", *Trans.* IEEE, AES-10, 5, Sep 1974 (717-718).
7. Weibull, W. "A Statistical Distribution Function of Wide Applicability", *J. Applied Mechanics*, 18, Sep 1951 (293-297).
8. Baker, J. D., "The Weibull Distribution as a Model for Radial Errors", *Navigation*, 14, 2, Summer 1967 (179-186).
9. Anderson, E. W., "Is the Gaussian Distribution Normal?", *J. Inst. Navigation*, 18, 1, Jan 1965 (65-71).
10. Plait, A., "The Weibull Distribution—with Tables", *Industrial Quality Control*, Nov 1962.
11. Gumbel, E. J., "Statistics of Extremes", Columbia Univ. Press, New York, 1958 (29-34).
12. Johnson, L. G., "The Median Ranks of Sample Values in their Population with an Application to Certain Fatigue Studies", *Industrial Mathematics*, 2, 1951 (1-9).
13. Menon, H. V., "Estimation of the Shape and Scale Parameters of the Weibull Distribution", *Technometrics*, 5, 2, May 1963 (175-182).

Appendix

The Weibull probability density function is defined as

$$pdf(X) = \frac{C}{B}\left(\frac{X-A}{B}\right)^{C-1} e^{-((X-A)/B)^C}$$

where

A = Location parameter $-\infty < A < +\infty$
B = Scale parameter, $B > 0$
C = Shape parameter, $C > 0$

For application to non-negative variates the location parameter is defined as $A = 0$, so that the *pdf* of radial error R in a navigational position fix is then

$$pdf(R) = \frac{C}{B}\left(\frac{R}{B}\right)^{C-1} e^{-(R/B)^C}$$

and the corresponding cumulative distribution function is

$$CDF(R) = \int_0^R pdf(R)dR = 1 - e^{-(R/B)^C}$$

The mean value of radial error is

$$\mu_R = \int_0^\infty R \cdot pdf(R) dR = B\Gamma\left(1+\frac{1}{C}\right)$$

where the Gamma Function

$$\Gamma(Z) = \int_0^\infty t^{z-1}e^{-t}\,dt$$

is available in tabular form.
The RMS value of radial error is

$$RMS_R = \sqrt{\int_0^\infty R^2 \cdot pdf(R)\,dR}$$

$$= B\sqrt{\Gamma\left(1+\frac{2}{C}\right)}$$

The variance of radial error is

$$\sigma_R^2 = RMS_R^2 - \mu_R^2$$

$$= B^2\left[\Gamma\left(1+\frac{2}{C}\right) - \Gamma^2\left(1+\frac{1}{C}\right)\right]$$

The "most probable value" (mode) value of radial error occurs where

$$\frac{d(pdf)}{dR} = 0$$

Most probable error

$$= B\left(1-\frac{1}{C}\right)^{1/C} \quad \text{for} \quad C > 1$$

$$= 0 \quad \text{for} \quad 0 < C \leq 1$$

The radius R_p that includes the p-th percentile of the distribution is found by setting $\text{CDF}(R_p) = p$. Hence

$$R_p = B[-\ln(1-p)]^{1/C}$$

Example: To find the CEP, set $p = 0.5$, yielding $R_{CEP} = B(0.693)^{1/C}$
If $C = 2$ (Rayleigh distribution), $R_{CEP} = 0.8326B$.